

M.B. DANAILOV¹,
A.A. DEMIDOVICH²
A.N. KUZMIN³
O.V. KUZMIN⁴
V.L. HAIT⁴

On the performance of short pulse Nd³⁺:LSB microchip lasers

¹ Laser Laboratory, Sincrotrone-Trieste, SS14, km.163.5, 34012 Trieste, Italy

² Institute of Molec. & Atom. Physics, F. Skaryna Ave. 70, 220072 Minsk, Belarus

³ Stepanov Inst. of Physics, F. Skaryna Ave. 70, 220072 Minsk, Belarus

⁴ STC FIRN, Starokubanskaya Str. 114, 350058 Krasnodar, Russia

Received: 11 June 2001/Revised version: 30 July 2001

Published online: 15 October 2001 • © Springer-Verlag 2001

ABSTRACT Experimental results from studies of the laser characteristics of Nd:LSB crystals in both cw and passive Q-switching arrangements are presented. The dependence of the main laser parameters on the output coupling and saturable absorber transmission for two doping levels of Nd was investigated. It is demonstrated that due to its high absorption, low losses and intrinsic strong thermal lensing, even at pump powers of less than 200 mW, the Nd:LSB has excellent properties in terms of efficiency, beam quality and pulse duration. In addition, it exhibits high pulse-to-pulse and pulse width versus pump power stability.

PACS 42.55.Xi; 42.60.Gd; 42.60.Lh

1 Introduction

Microchip lasers containing a saturable absorber (SA) Q-switch have been widely studied in the last decade [1]. In addition to their compactness and reliability, the potential for numerous scientific and practical applications is determined by the possibility to generate sub-nanosecond pulses with high peak power and excellent beam quality. The great majority of experimental and theoretical studies in the literature are dedicated to the Nd:YAG, which in combination with a Cr⁴⁺:YAG SA allows pulses of 300 ps duration and peak power of up to 0.5 MW to be achieved [1]. Although Nd:YAG is a very good material for microchip lasers, its relatively small absorption coefficient (12 cm⁻¹ for a typical 1% Nd³⁺ concentration) and narrow absorption band (< 1.5 nm) set stringent requirements on the spectrum of the pump diodes. In addition, as thermal lensing of the active material is essential for the stability of the microchip laser cavity (and given the relatively low pump light absorption), pump diodes in the 1 W range have to be used in the case of Nd:YAG for obtaining good performance. However, the use of higher gain materials like Nd:YVO₄, possessing a cross section comparable to the absorption cross section of Cr⁴⁺:YAG, requires the use of more complicated and longer resonators. This in general leads to longer pulses if a conventional SA is used [2].

A very promising material for compact Q-switched lasers is Nd:LSB [3–6]. The cw operation of this laser medium has been demonstrated with pump powers up to 5.6 W [3], however, due to its low thermal conductivity, Nd:LSB has the best lasing performance at low pump power. The LSB crystal allows doping with Nd³⁺ up to 50% without significant fluorescence quenching and keeping high optical quality. Crystals with 30% Nd doping and losses as low as 0.0003 cm⁻¹ are now available [4]. Even at 10% doping the Nd:LSB has an absorption coefficient three times higher than that of the standard (1%) Nd:YAG, and its absorption bandwidth is about 3 nm. These features have contributed to achieving very efficient performance, namely 64% slope efficiency in the cw regime [5] and passive Q-switching operation (using an anti-resonant Fabry–Perrot SA) with pulses as short as 180 ps [6]. Still, there is little literature data on the design and performance of compact Nd:LSB lasers at low pump power levels, especially in the regime of Q-switching.

In this paper we present results from studies of the laser characteristics of Nd:LSB crystals in both cw and passive Q-switching arrangements. The dependence of the main laser parameters on the output coupling and SA transmission for two doping levels are given. The emphasis is on Q-switched operation obtained by using a Cr:YAG saturable absorber. We demonstrate that even at low pump power Nd:LSB has excellent properties in terms of efficiency, pulse duration and beam quality. In addition, it exhibits low jitter and remarkable stability of the pulse width versus pump power. We attribute this good performance to the effective pump power absorption, low losses and intrinsically strong thermal lensing.

2 Experimental set-up

The experimental set-up is shown on Fig. 1. A 1 W diode with a 150 μm stripe (ATC SD, S. Petersburg) and built-in micro-lens was used as a pump source. The pump wavelength was temperature-tuned to the Nd:LSB absorption peak at 807.5 nm. The pump was focused by a triplet with a 10 mm focal length to an elliptical spot of dimensions 40 μm and 60 μm in the vertical and horizontal planes, respectively. A variable attenuator was placed between the diode and the focusing lens, allowing the pump power to be varied without affecting the pump distribution and spectrum. Two Nd:LSB crystal samples with 10% doping (1.2 mm thick) and

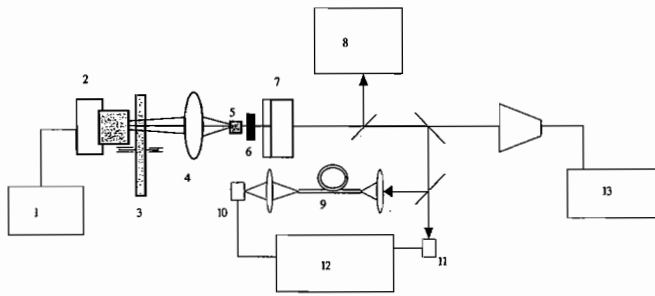


FIGURE 1 Scheme of the experimental set-up: 1 – laser driver and TEC controller; 2 – diode laser with microlens; 3 – variable attenuator; 4 – lens; 5 – Nd:LSB crystal; 6 – Cr:YAG crystal; 7 – output mirror; 8 – optical spectra analyzer; 9 – optical fiber delay line; 10, 11 – photodiodes; 12 – oscilloscope; 13 – power meter

30% doping (0.3 mm thick) were used. Both crystals were AR coated ($R \geq 0.1\%$) at 1062 nm on one face, while the coating on the other face had a high reflectivity ($R \geq 99.8\%$) at 1062 nm and high transmission ($T \geq 95\%$) at 808 nm. The crystals were mounted on a copper heat sink with a thermo-conductive compound. In the case of the 30% doped crystal, an additional transparent heat sink (undoped YAG plate) was attached to the surface with HR coating. The resonator components were mounted as close as possible (a total air gap about $300 \mu\text{m}$ was estimated) so that the cavity length was practically the sum of the active crystal and SA thickness. As a SA we used Cr^{4+} :YAG plates, AR coated at 1062 nm, with initial transmissions of 90%, 86%, 83%, 78%, thicknesses of 0.35 mm, 0.56 mm, 0.71 mm and 0.86 mm and estimated non-saturable losses of 2.5%, 3%, 3.5%, and 5%, respectively.

The average power, repetition rate and pulse duration were measured simultaneously. For the latter we used a 25 GHz pin photodiode (New Focus mod.1417) connected to a transient digitizer (Tektronix CSA 803C). To provide a properly anticipated trigger pulse, the main pulse was delayed by about 50 ns using 20 m of single mode fiber.

3 Experimental results

In order to characterize the quality of the available LSB crystals we first studied their performance in the cw regime. We measured the dependence of the output power versus pump power as a function of the output coupler reflectivity. In the case of a 30% doped Nd:LSB crystal, the maximum pump power was limited to 480 mW to avoid deformation and damage of the HR coating. We present in Fig. 2 the results for a 95% output coupling, which was found to be the optimum for both cases. As is seen, slope efficiencies of 64% and 53% and thresholds of 54 and 28 mW were obtained for the 10% doped and 30% doped Nd:LSB crystals, respectively. It is worth noting here that the crystal absorption depends on the pump power (see Fig. 3), which can be attributed to heating-induced redistribution of the population of the $^4I_{9/2}$ level and/or to decrease in the oscillator strength of the transition at increased temperature. From the measurements at different output couplings the passive cavity losses were estimated [7] to be of the order of 0.5%.

As was expected, due to its broad absorption band, the LSB performance was nearly independent of the laser diode

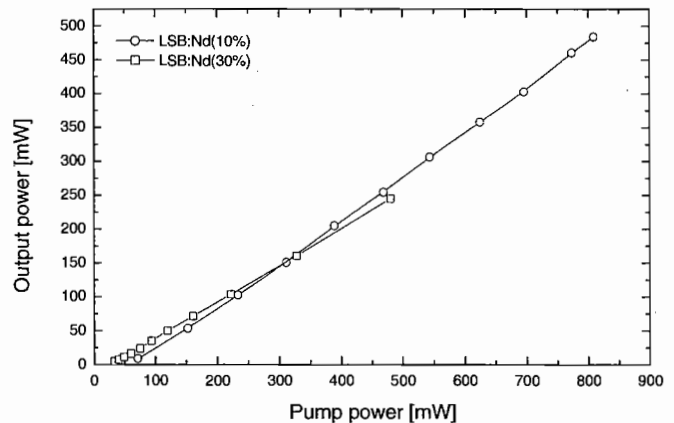


FIGURE 2 Output power of the 10% Nd:LSB and 30% Nd:LSB lasers in cw mode vs. pump power, 95% output coupler

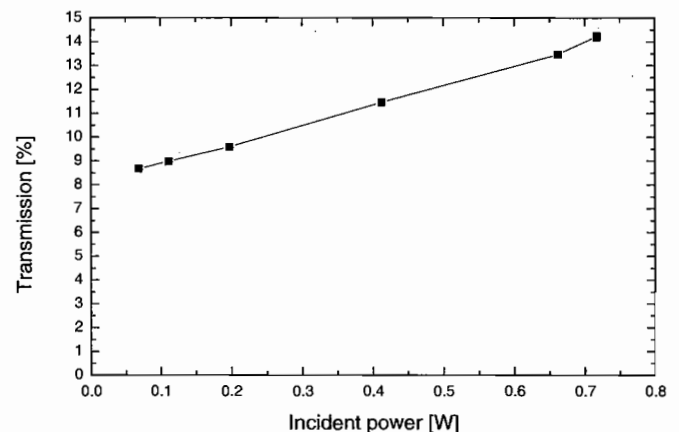


FIGURE 3 Transmission of the 10% Nd:LSB crystal (1.2 mm thickness) vs. incident power

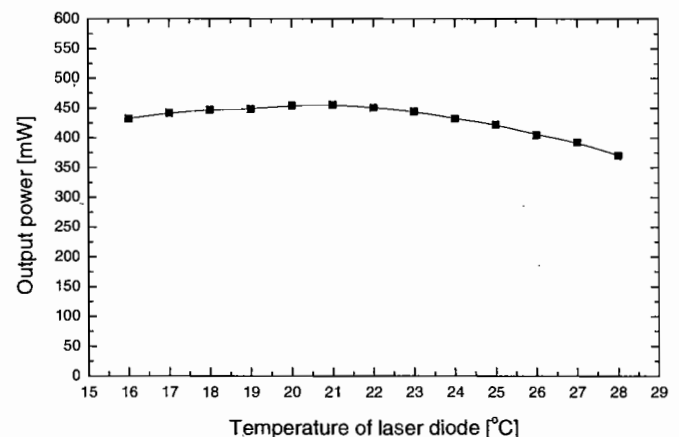


FIGURE 4 Output power of the 10% Nd:LSB laser in cw generation vs. LD temperature, pump power 810 mW

temperature. This is illustrated in Fig. 4 for the 10% doped crystal at 810 mW pump power. In this measurement, the diode temperature was changed in the range 16–28 °C, which corresponds to a pump wavelength change in the range of 806–809 nm.

In the range of pump power reported here the plane-plane cavity was made stable by the thermal lensing of the active material. By moving the output coupler, we found that at maximum pump power (800 mW), laser generation disappeared

at a cavity length of 5.8 mm. Taking into account the crystal thickness and refractive index [8], a thermal lens of about 6 mm focal length can be estimated.

Even if the cw operation of LSB is quite satisfactory, its main advantages are seen in the Q-switched regime. Using the set-up described above, we have tried to perform a complete investigation of the behaviour of the two active crystals using a number of saturable absorbers and output coupler mirrors. The first four groups of Fig. 5–8 present the average output power, repetition rate, pulse width and pulse energy of the Q-switched 10% Nd doped LSB laser versus pump power at different initial transmissions of the SA (90%, 86%, 83% and 78%). In Fig. 9, the same parameters are plotted for the 30% doped crystal with 90% SA. In each figure, the curves corresponding to different output couplers (OC) are presented. It is seen that some of the monitored parameters have nearly monotonic behaviour with respect to both output coupling and initial transmission of the SA. For example, the pulse width decreases with decreasing initial transmission of the absorber

and with increasing mirror transmission, and is very weakly dependent on the pump power. Also, the maximum average power (obtained with the optimum OC and at maximum pump power) is a decreasing function of the SA initial transmission, and the repetition rate at a given output coupling and SA increases with pump power. In contrast, the measured behaviour of the pulse energy versus pump power output coupling and SA value appear to be difficult to generalize. Comparison of Fig. 5c and 9c shows that if the same SA and output coupler are used, the shorter, highly doped crystal allows the generation of shorter pulses. For example, with 90% OC and 89% SA at 480 mW pump power, pulse durations of 1.22 ns and 0.95 ns were measured with the 10% doped and 30% doped crystals, respectively. We expect that by being properly cooled and pumped at 800 mW, the latter crystal will allow lasing with higher SA and OC transmission, and sub-500 ps pulse generation can be expected.

As the shortest obtainable pulse duration is of interest in many cases, we present an additional graph (Fig. 10), where

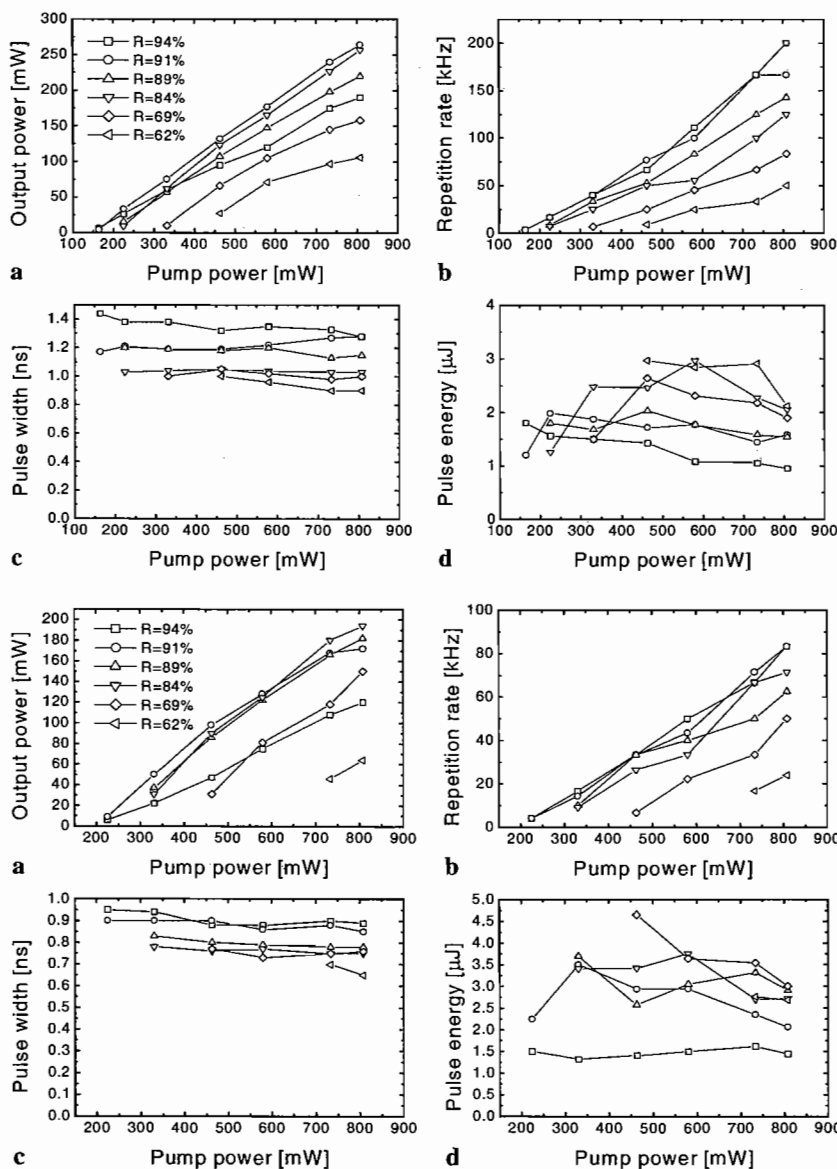


FIGURE 5 Average output power (a), repetition rate (b), pulse width (c), and pulse energy (d) of the Q-switched 10% Nd:LSB laser vs. pump power, 90% SA and different output coupler reflectivity

FIGURE 6 Average output power (a), repetition rate (b), pulse width (c), and pulse energy (d) of the Q-switched 10% Nd:LSB laser vs. pump power, 86% SA and different output coupler reflectivity

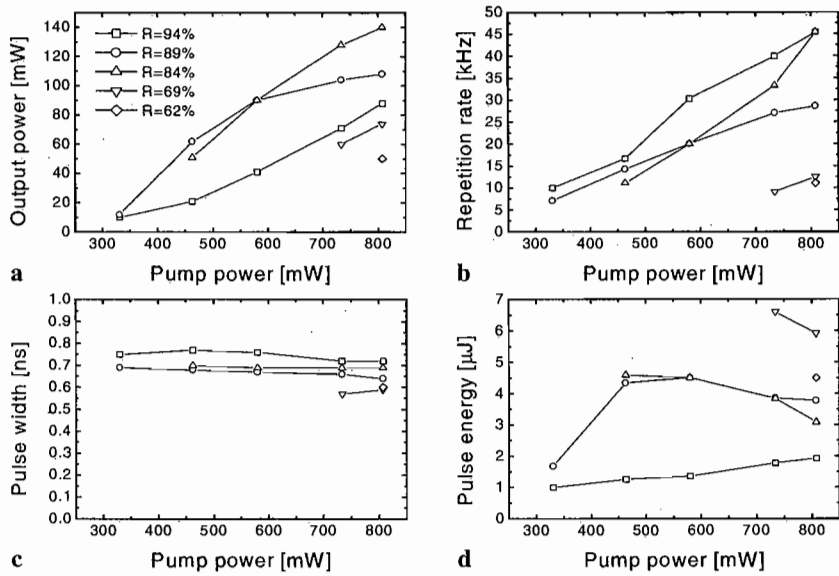


FIGURE 7 Average output power (a), repetition rate (b), pulse width (c), and pulse energy (d) of the Q-switched 10% Nd:LSB laser vs. pump power, 83% SA and different output coupler reflectivity

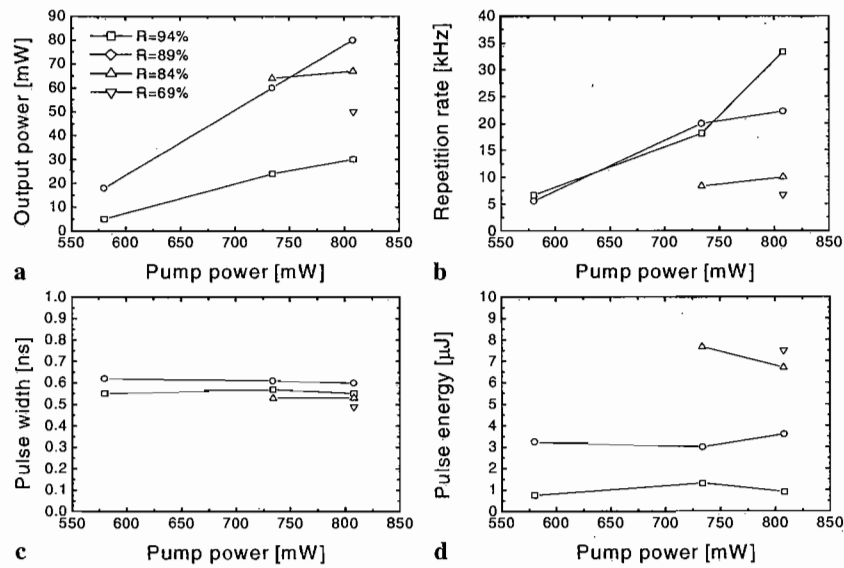


FIGURE 8 Average output power (a), repetition rate (b), pulse width (c), and pulse energy (d) of the Q-switched 10% Nd:LSB laser vs. pump power, 78% SA and different output coupler reflectivity

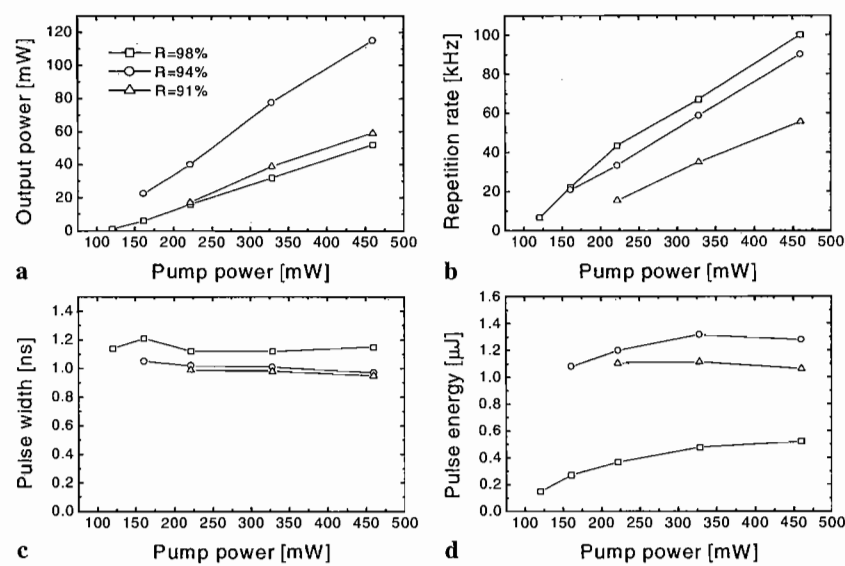


FIGURE 9 Average output power (a), repetition rate (b), pulse width (c), and pulse energy (d) of the Q-switched 30% Nd:LSB laser vs. pump power, 90% SA and different output coupler reflectivity

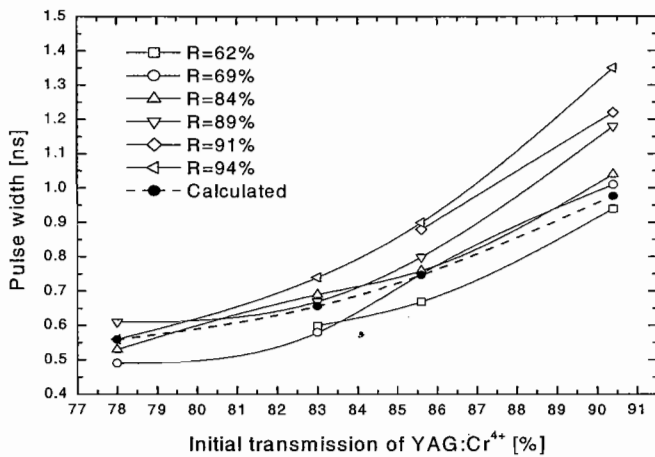


FIGURE 10 Pulse width of the Q-switched 10% Nd:LSB laser vs. initial SA transmission at different output coupler reflectivity

pulse duration obtained with the 10% doped crystal is plotted against the SA transmission and the output coupling. In Fig. 11 we show a typical oscilloscope trace of the Q-switched 10% Nd:LSB laser at 83% SA and 69% output coupler reflectivity. Pulse length is 580 ps FWHM.

Concerning the pulse duration, we should like to point out that it also depends on the SA orientation. This fact has been already reported in [9] for a relatively long cavity Nd:YVO₄ laser (24 mm), but to our knowledge there is no data in the literature on the influence of SA orientation on the pulse duration of microchip laser. In Fig. 12, the pulse duration for the case of 84% OC and 83% SA is plotted versus the SA rotation angle with respect to an arbitrary plane (it was verified that the plane of polarisation of the generated beam remains unchanged). As is seen, the pulse duration differs by 15% in the two orthogonal directions. The effect can be attributed to the change in the saturation intensity of the SA for different polarizations [9].

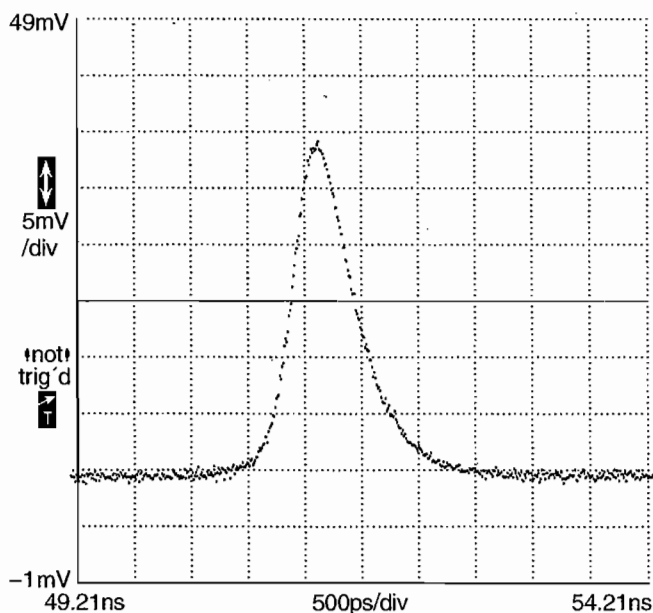


FIGURE 11 Typical oscilloscope trace for the Q-switched 10% Nd:LSB laser, 83% SA, 69% output coupler reflectivity

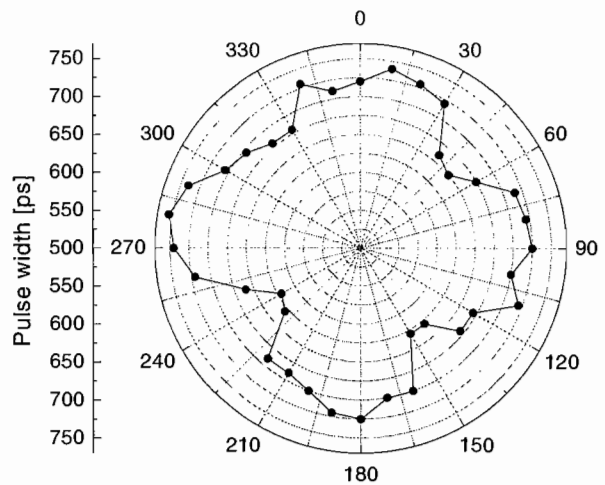


FIGURE 12 Pulse width of the 10% Nd:LSB laser vs. SA orientation

A logical question is whether the presented data agree with the predictions of the different models of Q-switched lasers [10, 11]. A detailed study of this point goes beyond the scope of this paper and we will only address two related works. We have compared pulse energy and pulse duration in some cases with the formulae and parametric graphs given in [11]. Using their typical Nd:LSB parameters, namely a stimulated emission cross section (σ) of $1.3 \times 10^{19} \text{ cm}^2$ and an inversion reduction factor (γ) of 0.63, and assuming equal beam size in the active and SA crystals and equal pump and lasing mode size, one obtains 0.5–2 ns for the pulse duration and 2–15 μJ for the energy, in relatively good agreement with our measurements. It is interesting also to compare our measurements with the results from an approximated expression for the pulse duration given in [10]: $\tau_p \approx 3.52 T_r/q_0$. Here T_r is the cavity round-trip time and q_0 is the modulation depth, assumed to be equal to the total non-saturable round trip loss coefficient l . When our cavity length and modulation depth with different saturable absorbers are substituted in the above expression, the curve presented by filled circles and the dashed line in Fig. 10 is obtained. Comparing with the measured data (for each SA, the value measured with the output coupler which is closest to the condition $q_0 = l$ must be taken) it is seen that the formula gives reasonably good agreement with our measurements, especially at high modulation depth. We recall that in related works [10, 12] discrepancies of nearly 50% between measured and calculated pulse duration have been observed.

We also measured the spectrum of the Nd:LSB laser in both cw and Q-switching modes. The cw spectrum is always multimode and about 1 nm wide at FWHM. In the Q-switched regime, at low pump power (up to about 2 times above the threshold) a single-mode operation is observed. At higher power, the single pulse spectrum is still single-mode (solid line in Fig. 13), but the central wavelength of this mode may vary from pulse to pulse and the spectrum averaged over a large number of pulses exhibits up to 4 modes (dashed line, 300 pulses on Fig. 13).

As in many cases (e.g. harmonic generation), the spatial beam profile is important. In Fig. 14 we also present a typical spatial beam profile measured using a moving slit at

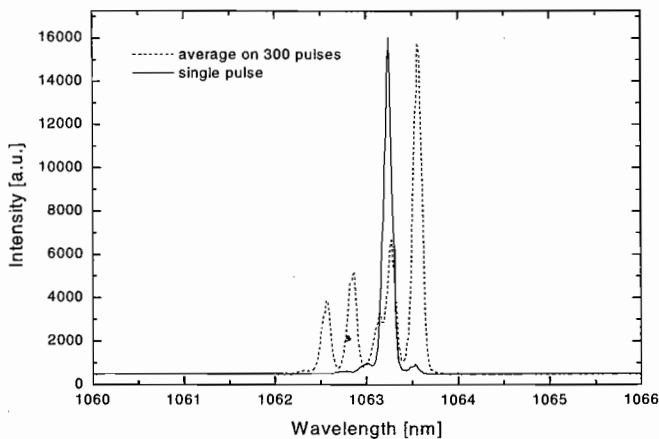


FIGURE 13 Spectra of the Q-switched 10% Nd:LSB laser

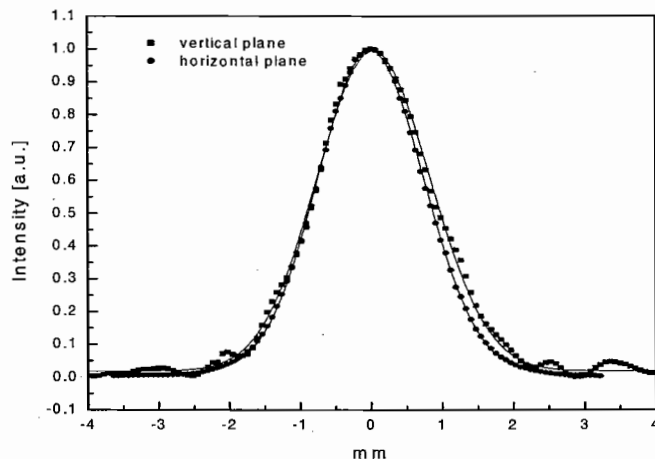


FIGURE 14 Spatial beam profile of the Q-switched 10% Nd:LSB at 140 mm distance from the laser. Experimental data (dots) and Gaussian fit (lines)

140 mm from the laser, with the 10% doped LSB crystal in a Q-switched regime at 810 mW pump power. As is seen, the far-field beam profile is well fitted by a Gaussian profile having a $1/e^2$ radius of 1.6 mm. This value indicates that the TEM₀₀ resonator mode radius on the OC mirror is about 30 μm , which is in good agreement with our previous estimation of the thermal lens focal length in cw mode.

4 Conclusions

The studies of the performance of diode-pumped Nd:LSB crystals in short cavity configuration presented in this paper indicate that it is a very convenient material for low pump power, short pulse (sub-nanosecond) lasers. It is

demonstrated that at very low pump power, (170 mW) pulses with a duration of 1.2 ns and pulse energy of 1.8 μJ can be generated. The shortest pulses (490 ps), with an energy of 8 μJ , were obtained at 800 mW pump power. The main advantage of the LSB is the combination of its high absorption, good optical quality and high thermal lensing. While the last property can be a serious drawback in high power systems, at very low pump power it provides stable cavity operation with small mode size, allowing for easy bleaching of the absorber and very stable, single pulse operation. Our experience is that in this regime the Nd:LSB works much better than commonly available 1.1% doped Nd:YAG and 3% doped Nd:YVO₄ crystals. There is a literature report demonstrating superior performance of a 1.8% doped Nd:YAG laser with pulses as short as 337 ps and energy of up to 11 μJ at 1.2 W pump power [12]. A direct comparison of the latter with the Nd:LSB performance presented here is not straightforward since pump power and spot size, as well as saturable absorber doping and cavity construction are different. Referring to pulse duration, we note that a two-fold pulse shortening is feasible in our set-up by using a cavity with shorter Nd:LSB and SA crystals. We believe that the data presented in this paper can be useful for the design and development of reliable and simple sub-nanosecond (and even sub-500 ps) lasers for various applications.

ACKNOWLEDGEMENTS

The work was supported by the High-Tech & New Materials Area of the International Centre for Science and High Technology (ICS), Trieste, Italy. Authors are grateful to Prof. G. Denardo for his constant help and encouragement.

REFERENCES

- 1 J.J. Zayhowski, C. Dill III, C. Cook, J.L. Daneu: In *Advanced Solid State Lasers*, Vol. 26 (Optical Soc. of America, Washington, DC 1999) p. 178
- 2 Y. Bai, N. Wu, J. Li, S. Li, J. Xu, P. Deng: *Appl. Opt.* **36**, 2468 (1997)
- 3 V.G. Ostroumov, F. Heine, S. Kueck, G. Huber, V.A. Mikhailov, I.A. Shcherbakov: *Appl. Phys. B* **64**, 301 (1997)
- 4 B. Chai, K. Petermann, G. Huber: *CLEO/Europe'96 Technical Digest* (IEEE Hamburg 1996) p. 76
- 5 B. Beier, J.P. Meyn, R. Knappe, K.J. Boller, G. Huber, R. Wallenstein: *Appl. Phys. B* **58**, 381 (1994)
- 6 B. Braun, F.X. Kärtner, U. Keller, J.P. Meyn, G. Huber: *Opt. Lett.* **21**, 405 (1996)
- 7 J.P. Meyn, G. Huber: *Opt. Lett.* **19**, 1436 (1994)
- 8 V. Magni: *Appl. Opt.* **25**, 107 (1986)
- 9 I.V. Klimov, V.B. Tsvetkov, I.A. Shcherbakov, J. Bartschhke, K.J. Boller, R. Wallenstein: In *Advanced Solid State Lasers*, Vol. 1 (Optical Soc. of America, Washington, DC 1996) p. 172
- 10 G.J. Spühler, R. Rascholta, R. Fluck, B. Braun, M. Moser, G. Zang, E. Gini, U. Keller: *J. Opt. Soc. Am.* **16**, 376 (1999)
- 11 X. Zang, S. Zhao, Q. Wang: *J. Opt. Soc. Am.* **17**, 1166 (2000)
- 12 J.J. Zayhowski, C. Dill III: *Opt. Lett.* **19**, 1427 (1994)